

Dioxygen and nitric oxide reactivity of a reduced heme/non-heme diiron(II) complex $[(^5L)Fe^{II}\cdots Fe^{II}-Cl]^+$. Using a tethered tetraarylporphyrin for the development of an active site reactivity model for bacterial nitric oxide reductase

Telvin D. Ju^a, Amina S. Woods^c, Robert J. Cotter^c, Pierre Moënne-Loccoz^b,
Kenneth D. Karlin^{a,*}

^a Department of Chemistry, The Johns Hopkins University, Charles and 34th Streets, Baltimore, MD 21218, USA

^b Department of Biochemistry and Molecular Biology, Oregon Graduate Institute of Science and Technology, Portland, OR 97291, USA

^c Department of Pharmacology and Molecular Sciences, The Johns Hopkins School of Medicine, Baltimore, MD 21205, USA

Received 20 May 1999; accepted 10 September 1999

Abstract

We present here a first-generation model and initial reactivity (with O₂ and NO) study for the heme/non-heme diiron active site chemistry of nitric oxide reductase (NOR), a denitrifying bacterial enzyme which converts nitric oxide to nitrous oxide (2NO + 2e⁻ + 2H⁺ → N₂O + H₂O). This research is also pertinent because of the considerable recent biological, chemical and industrial interest in NO and nitrogen oxides. The study employs the binucleating ligand ⁵L, with tetradentate tris(2-pyridylmethyl)amine (TMPA) chelate tethered to a tetraarylporphyrin (with three 2,6-difluorophenyl *meso* substituents). The new, reduced, diiron(II) compounds $[(^5L)Fe^{II}\cdots Fe^{II}-Cl]^+$ (**2**) have been synthesized by dithionite reduction of the previously characterized μ -oxo complex $[(^5L)Fe^{III}-O-Fe^{III}-Cl]^+$ (**1**) and characterized as either a perchlorate (from **2a**; λ_{max} 424 (Soret), 544 nm, tetrahydrofuran (THF)) or tetraarylborate (**2b**; BAr^F) anion complexes. NMR spectroscopic studies indicates **2** possesses a high-spin heme in non- or weakly coordinating solvents (CH₂Cl₂ or THF), and the evidence suggests that coordination from one of the pyridyl arms of the TMPA tether is involved. Reaction of **2** with O₂ results in the generation of an intermediate which is relatively stable at -80°C in THF (λ_{max} ; 416 (Soret), 538 nm), hypothesized to be a peroxo-bridged heme/non-heme diiron(III) complex. Warming of this intermediate gives back **1**. The reaction course of **2** with nitric oxide depends on the concentration. On a UV-Vis scale (< 10 μ M), a low-temperature stable intermediate (from **2a** (THF); λ_{max} 414 (Soret), 548 nm) forms, which upon warming gives the μ -oxo complex **1**, and presumably produces nitrous oxide. At higher concentrations, gas chromatographic analysis shows that both N₂O and NO₂ are produced, while UV-Vis, NMR, infrared and resonance Raman spectroscopic evidence indicates that a new red metal complex product obtained contains a iron(II)-nitrosyl moiety. This air-sensitive compound also reverts to **1** upon exposure to O₂. Discussion includes reference to nitric oxide reductase (NOR) chemistry, and suggestions for the mechanism(s) of the observed reactions and product NO_x formation. © 2000 Elsevier Science S.A. All rights reserved.

Keywords: Diiron(II) complexes; Bacterial nitric oxide reductase; Metal-nitrosyl complexes; Iron(II)-nitrosyl moiety; NOR chemistry; Tetraarylporphyrin

1. Introduction

Abbreviations: NOR, nitric oxide reductase; CcO, cytochrome *c* oxidase; TMPA, tris(2-pyridylmethyl)amine; BAr^F, tetrakis(3,5-bis-trifluoromethyl-phenyl)borate; MALDI-TOF-MS, matrix assisted laser desorption ionisation time of flight mass spectrometry; por, porphyrin; THF, tetrahydrofuran; GC, gas-chromatography.

* Corresponding author.

Denitrification, the reduction of nitrate to dinitrogen, consists of four distinct steps: NO₃⁻ → NO₂⁻ → NO → N₂O → N₂ [1,2]. Historically, there has been considerable interest in this process due to its importance in the global nitrogen cycle. More recently, nitrate has been

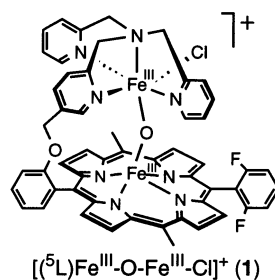
attributed as a pollutant to ground- and surface-water, NO is detrimental in ozone chemistry, and N₂O has been identified as a major greenhouse gas [1]. These environmental issues have led to increased attention and research efforts in the chemistry of these species.

In bacterial denitrification, nitrogen oxides are utilized as terminal electron acceptors in electron transport phosphorylation to harvest energy for metabolic functions, predominately under anaerobic conditions [1]. The enzyme responsible for the reduction of NO to N₂O is nitric oxide reductase (NOR). It was the last enzyme to be identified among the four enzyme systems involved in bacterial denitrification and is thus somewhat less well characterized [3]. Nevertheless, NOR is now known to be a membrane-bound cytochrome *bc* complex, containing 2 sub-units (NorB and NorC), that catalyzes the reduction of two NO molecules into N₂O and water. The two electrons required in this process are donated by cytochrome *c* [4].

NOR isolated from *Paracoccus denitrificans* [1,5] was shown to contain a stoichiometry of one high- and one low-spin heme *b*, one low-spin heme *c*, and one non-heme iron per enzyme. Structural studies have shown that the larger of the two sub-units, NorB, contains binding sites for the two heme *bs* and the non-heme iron [1]. From resonance Raman [6], EPR [4,7,8], and MCD [8] studies, it has been concluded that the active form of NOR reacting with NO is a reduced dinuclear iron(II) center and comprises the high-spin heme *b* and the non-heme iron. Moreover, NorB exhibits a high sequence homology to that of sub-unit I of cytochrome *c* oxidase (*CcO*), and the six histidine residues that ligate heme *a*, heme *a*₃, and Cu_B in *CcO* are conserved in NorB [1]. From these observations it has been suggested that NOR and *CcO* are evolutionarily related enzymes (with *CcO* evolving from NOR) and that the non-heme iron in NOR occupies the exact same position of Cu_B in *CcO* [1]. In addition, NOR from *Paracoccus denitrificans* was found to reduce dioxygen [3,9], and *CcO* has been long known [10] to reduce NO to N₂O at a much slower rate than NOR [8] (albeit new evidence suggests that under anaerobic conditions *CcO* does not catalyze the reduction of NO [11]), therefore providing further support to the suggestion of the close relation between *CcO* and NOR.

As part of our research program to model the heme-Cu active site chemistry of *CcO*, we have been developing chemistry which employs binucleating ligands having a heme along with a tethered chelate which can bind another metal such as copper [12–14]. Initial use of the ligand ⁵L (with tetradentate TMPA tethered to a porphyrin periphery) resulted in our isolation and characterization of the diiron complex [(⁵L)Fe^{III}-O-Fe^{III}-Cl](ClO₄) (**1a**) [15]. Recent biophysical studies [6,8] have led to suggestions that such a μ-oxo heme/non-heme diiron(III) moiety (or perhaps a proto-

nated μ-OH⁻ analog) may be present in the NOR active site resting (oxidized) state, and this may even represent a reaction turnover intermediate. Thus, complex **1** can be considered a first generation NOR structural mimic.



Here, we wish to report the synthesis and characterization of related reduced complexes, [(⁵L)Fe^{II}...Fe^{II}-Cl]⁺ (**2**) (as ClO₄⁻ or BAr^F⁻ salts, which may thus serve as an NOR active-site mimic for the functionally reactive form poised for nitric oxide binding and reduction. In developing models to provide insights into NOR reaction mechanism, the reactivities of this complex with nitric oxide, as well as dioxygen, will also be described.

2. Experimental

2.1. Materials and methods

Commercially available reagents and solvents were used without further purification, unless stated otherwise. Dichloromethane (CH₂Cl₂) was distilled from CaH₂ under Ar. Tetrahydrofuran (THF) was distilled over sodium/benzophenone under Ar. Propionitrile (C₂H₅CN) was first distilled over P₂O₅, then refluxed and distilled over CaH₂. All solvents were deoxygenated by bubbling Ar directly through the solution and followed by two cycles of freeze–pump–thaw. Deuterated solvents were distilled according to standard procedures and deoxygenated by at least three cycles of freeze–pump–thaw. Glassware was flame-dried under vacuum prior to use. Air-sensitive manipulations were carried out with rigorous exclusion of dioxygen using standard Schlenk techniques under an atmosphere of Ar or in a MBraun Labmaster 130 Vacuum/Atmospheres glovebox under nitrogen. Nitric oxide of research purity was purchased from MG Industries, and purified by passage through two traps cooled by: 1. acetone/dry ice (−78°C), 2. hexane/liquid nitrogen (−94°C), and followed by passage through a P₂O₅ column. Labeled ¹⁵N¹⁸O was purchased from ICON (isotopic purity: ¹⁵N — 99.9%, ¹⁸O — 99.4%) and used without further purification.

Infrared spectra were recorded on a Mattson Galaxy 4030 FT-IR spectrometer. Solution IR spectra were obtained using a CaF₂ windowed cell. NMR spectra were measured on a Bruker 300 MHz NMR instrument or a Varian NMR instrument at 400 MHz. All spectra were recorded in airtight 5 mm o.d. screw cap NMR tubes fitted with septum purchased from Wilmad, and chemical shifts are reported as δ values downfield from an internal standard of Me₄Si (¹H), as δ values referenced from solvent peaks, or as δ values referenced to an external standard of α,α,α -trifluorotoluene at -63.73 ppm (¹⁹F). UV-Vis spectroscopy was recorded either with a Shimadzu UV160U diode array spectrophotometer or at low temperature with a Hewlett-Packard 8452A diode array spectrometer driven by a Gateway computer with software written by OLIS, Inc. The spectrometer was equipped with a variable-temperature Dewar as described elsewhere [16]. Specially designed cuvettes fitted with Schlenk joints were used to obtain the UV-Vis spectra. Gas chromatography was performed on a Hewlett-Packard 5890 series II gas chromatograph using a HP-5 column (cross-linked 5% Ph Me Silicone, dimension 30 m \times 0.53 mm \times 0.88 μ m, 30 ml min⁻¹ flow rate with the initial temperature at 30°C, and a heating rate of 0.5°C min⁻¹) and equipped with a thermal conductivity detector. Resonance Raman spectra were obtained as previously described [6]. Samples were prepared by dissolving the reduced complex to be studied in THF in an NMR tube and bubbling them with O₂ at -80°C . Matrix assisted laser desorption ionization time of flight (MALDI-TOF-MS) mass spectra were recorded on a Kratos Analytic Kompact MALDI 4 mass spectrometer equipped with a 337 nm nitrogen laser (20 kV extraction voltage).

2.2. Syntheses and procedures

2.2.1. Synthesis of [(⁵L)Fe^{III}-O-Fe^{III}-Cl](ClO₄) (**1a**)

This compound was synthesized according to the literature [15]. A typical procedure is as follows: under Ar, 450 mg (0.43 mmol) of ⁵L was dissolved in deoxygenated DMF (30 ml) in a 100 ml Schlenk flask, and the solution was taken to reflux. Then, 1.027 g (8 mmol, 18 equiv.) of FeCl₂ was added under Ar and the reaction mixture was heated at reflux for an additional 2 h, at which time the solution turned a dark reddish color. Subsequently, the solution was allowed to cool to room temperature (r.t.) while exposed to air. The solution at this point had turned to a more intense red. Once cooled, saturated NaCl (20 ml) solution was added to the mixture, resulting in the formation of a brown precipitate. The mixture was placed at -20°C overnight. The reaction mixture was filtered through a Celite plug (5 cm) to remove the precipitate, and the plug was subsequently washed with water until the

washings were colorless. The Celite plug with the precipitate was dried under vacuum, and then washed with CH₂Cl₂ to remove the absorbed material. The organic layer was dried over Na₂SO₄ for 1 h, and then the solid was removed by filtration. The solvent was removed by rotary evaporation and the product at this point was believed to be [(⁵L)Fe^{III}-O-Fe^{III}-Cl](Cl). This solid was dissolved in CH₃CN (30 ml), and combined with a separately prepared solution of CH₃CN (5 ml) containing 0.1 g of NaClO₄. (**Caution:** NaClO₄ is explosive if handled incorrectly, care must be taken when using this reagent).

The solution was stirred for 1 h, then filtered through a Celite plug and washed with CH₃CN (3 \times 20 ml), and finally the solvent was removed on the rotary evaporator. This crude product was purified by column chromatography (1.5 cm \times 15 cm, neutral alumina) with methanol in CH₂Cl₂ gradient (2–5%). The procedure yielded 0.2 g (35% yield from ⁵L) of pure product. *R*_f (alumina, 5% methanol/CH₂Cl₂) = 0.25. UV-Vis (CH₂Cl₂), λ_{max} : 413 (Soret), 567 nm. ¹H NMR (300 MHz, CDCl₃, ppm): 22–20 (br, methylene CH₂ and PY-6H), 15.8 (br, pyrrole-H), 15.21, 12.4 (PY-3H and PY-5H), 7.6 (phenyl-H).

2.2.2. Synthesis of [(⁵L)Fe^{III}-O-Fe^{III}-Cl](BAR^F) (**1b**)

An identical procedure (as above) was followed in order to synthesize [(⁵L)Fe^{III}-O-Fe^{III}-Cl](Cl). At this point, 350 mg (0.28 mmol) of crude material was dissolved in a 100 ml round bottom flask with CH₃CN (30 ml). Then 290 mg of NaBAR^F (0.33 mmol, 1.16 equiv.), prepared as described in the literature [17], was added to the solution and allowed to stir overnight. The solution was filtered over Celite to remove insoluble salts and the Celite was washed with CH₃CN (2 \times 10 ml). The organic solvent was removed by rotary evaporation to yield a purplish solid. This solid was further purified by column chromatography (neutral alumina, first with CH₂Cl₂, then switched to 0.5% methanol/CH₂Cl₂ over a gradient). The procedure yielded 100 mg (7% yield from ⁵L) of purple solid. *R*_f (alumina, 1% MeOH/CH₂Cl₂) = 0.18. UV-Vis spectroscopy (CH₂Cl₂, λ_{max}): 413 nm (Soret), and 567 nm. IR (Nujol): 1463, 1377, 1354, 1277, 1124, 997 cm⁻¹. ¹H NMR (CDCl₃, 300 MHz) representative peaks: δ 22–20 (br, methylene CH₂ and PY-6H), 15.72 (br, pyrrole-H), 15.14, 12.3 (PY-3H and PY-5H), 11.53 [11]. ¹⁹F NMR (CD₂Cl₂, 400 MHz): δ -63.4 (s, sharp, BAR^F), -106 – 9 (m, br, TPP-fluorine), integration BAR^F⁻: TPP-F = 4:1.

2.2.3. Synthesis of [(⁵L)Fe^{II}...Fe^{II}-Cl]⁺

[(⁵L)Fe^{II}...Fe^{II}-Cl](ClO₄) (**2a**) and [(⁵L)Fe^{II}...Fe^{II}-Cl](BAR^F) (**2b**) were prepared following the same procedure of reduction with sodium dithionite as described elsewhere for the synthesis of [(⁵L)Fe^{II}...Cu^I](BAR^F)

[13]. An example is as follows: under Ar, a solution of $[(^{55}\text{L})\text{Fe}^{\text{III}}\text{-O-Fe}^{\text{III}}\text{-Cl}](\text{ClO}_4)$ (**1a**) (110 mg, 0.08 mmol) in deoxygenated CH_2Cl_2 (90 ml) was added to a 1 M solution of sodium dithionite in deoxygenated water (40 ml). The two solutions were mixed thoroughly with Ar bubbling for 30 min, at which time the color of the organic layer had changed from a dark red–brown to an intense red. The organic layer was separated from the aqueous layer, and the solvent was removed in vacuo to produce a purple–red solid (80 mg, 75%). UV–Vis spectroscopy of $[(^{55}\text{L})\text{Fe}^{\text{II}}\cdots\text{Fe}^{\text{II}}\text{-Cl}](\text{ClO}_4)$ (**2a**) (THF): $\lambda_{\text{max}} = 424$ (Soret) and 544 nm; ($\text{C}_2\text{H}_5\text{CN}$): $\lambda_{\text{max}} = 422$ (Soret) and 532 nm; and $[(^{55}\text{L})\text{Fe}^{\text{II}}\cdots\text{Fe}^{\text{II}}\text{-Cl}](\text{BAr}^{\text{F}})$ (**2b**) (THF): $\lambda_{\text{max}} = 424$ (Soret) and 549 nm. IR of **2a** (Nujol): 1462, 1261, 1099, 1018, 798 cm^{-1} . Solution IR of **2b** in THF: 1463, 1354, 1279, 1163, 1129 cm^{-1} . ^1H NMR of **2a** ((300 MHz, THF- d_8 , ppm): 53–58 (m, pyrrole). ^1H NMR of **2b** ((300 MHz, THF- d_8 , ppm): 57 (m, pyrrole), 28 (s, pyrrole)). ^1H NMR of **2b** ((300 MHz, CD_2Cl_2 , ppm): 28.7 (s), 28.9 (s), 30.2 (s), 30.6 (s) — all pyrrole). ^{19}F NMR spectroscopy of $[(^{55}\text{L})\text{Fe}^{\text{II}}\cdots\text{Fe}^{\text{II}}\text{-Cl}](\text{ClO}_4)$ (**3**) shows two sets of peaks all belonging to TPP-F: ((400 MHz, THF- d_8 , ppm): the first set appears at -108.11 (br, s, integration = 1:1 for this set), and -108.76 (br, s). The second set appears at -112.97 (sh, s, integration = 1:2:1 for this set), -113.39 (sh, s), and -113.80 (sh, s)). **2b** ((400 MHz, THF- d_8 , ppm): -65.3 (s, $\text{BAr}^{\text{F}-}$), -104 (br, TPP-F), -105 (br, TPP-F), integration ($\text{BAr}^{\text{F}}:\text{TPP-F}$) is 4:1). MALDI–TOF–MS for both compounds show a peak at $m/z = 1186$, corresponding to the species $[(^{55}\text{L})\text{Fe}^{\text{II}}\cdots\text{Fe}^{\text{II}}\text{-Cl}]^+$ ($M - \text{BAr}^{\text{F}-}$) $^+$ and $(M - \text{ClO}_4^-)^+$.

2.2.4. Reaction of $[(^{55}\text{L})\text{Fe}^{\text{II}}\cdots\text{Fe}^{\text{II}}\text{-Cl}]^+$ (**2a** and **2b**) with dioxygen, by UV–Vis spectroscopy

Typically, a dilute stock solution ($< 10 \mu\text{M}$) was made up by dissolving a few crystals of solid in THF (5 ml) in the glove box. This solution was transferred to a cuvette assembly, diluted with THF to the concentration desired, and removed from the glove box. The solution was cooled to -80°C and a UV–Vis spectrum recorded. Next, dioxygen was added directly to the solution through a syringe and the spectrum taken again. The cuvette was warmed to r.t., and was re-cooled to -80°C before the UV–Vis spectrum was again recorded, in order to follow the reaction to completion.

2.2.5. Reaction of $[(^{55}\text{L})\text{Fe}^{\text{II}}\cdots\text{Fe}^{\text{II}}\text{-Cl}]^+$ (**2a** and **2b**) with dioxygen followed by ^1H NMR spectroscopy

For ^1H NMR spectroscopy, typically 20 mg of solid was transferred to an air-free NMR tube and the solvent added to the sample, all performed in the glove box. The tube was then sealed with a screw cap and taken out of the glove box. After the spectrum of

the reduced complex was obtained, the sample was exposed to oxygen at r.t., either by injecting dioxygen using a syringe through the septum or by unscrewing the cap. The solution was then shaken to allow complete mixing. The spectrum of the oxidized complex was taken after an obvious color change (from an intense red to a reddish brown) had occurred.

2.2.6. Reaction of $[(^{55}\text{L})\text{Fe}^{\text{II}}\cdots\text{Fe}^{\text{II}}\text{-Cl}]^+$ (**2a** and **2b**) with nitric oxide at low complex concentration

A solution of low complex concentration, i.e. $< 10 \mu\text{M}$, was prepared in the glove box by adding a few milligrams of compound to 5 ml of THF. Some of this solution was transferred to an UV–Vis air-free cuvette assembly. The cuvette was then removed from the box, cooled to -80°C , and a spectrum recorded. The inert atmosphere was evacuated from the cuvette headspace and replaced with purified NO. The cuvette was shaken periodically under NO for 30 min at -80°C , after which time the excess NO was removed in vacuo and the UV–Vis spectrum taken again. The solution was warmed to r.t. and the UV–Vis spectrum of the solution was again recorded.

2.2.7. Reaction of $[(^{55}\text{L})\text{Fe}^{\text{II}}\cdots\text{Fe}^{\text{II}}\text{-Cl}]^+$ (**2a** and **2b**) with nitric oxide at higher complex concentration and isolation of product

In this case, stock solutions employed were ≥ 0.1 mM to allow for GC analysis of the head space of the flask for gaseous products formed during the reaction. A typical experiment consisted of dissolving 100 mg of $[(^{55}\text{L})\text{Fe}^{\text{II}}\cdots\text{Fe}^{\text{II}}\text{-Cl}](\text{ClO}_4)$ (**2a**) in 400 ml of THF (0.19 mM) in a 500 ml Schlenk flask in the glove box. The flask was charged with a stirrer and stoppered with a septum. Once outside, the flask was cooled to -80°C with stirring. The flask was then evacuated to remove the inert atmosphere and placed under a purified NO atmosphere for 30 min with stirring (the head-space of the flask was monitored by GC throughout the experiment to ensure that N_2O or NO_2 was not produced by disproportionation of NO). At this time the excess NO was removed and the flask warmed to r.t. Gaseous samples taken from the head-space were then checked by GC for products. Calibration of the GC instrument for NO_2 and N_2O was performed by injecting individual samples of NO_2 and N_2O into the GC and their times of elution, under identical conditions as that of the experiment, were noted. A UV–Vis spectrum of the solution was obtained following the GC studies. Heptane was then added to the solution under Ar, and a red powder-like solid was precipitated and isolated. The UV–Vis spectrum of this solid redissolved in THF was identical to that of the solution from which it was isolated.

3. Results and discussion

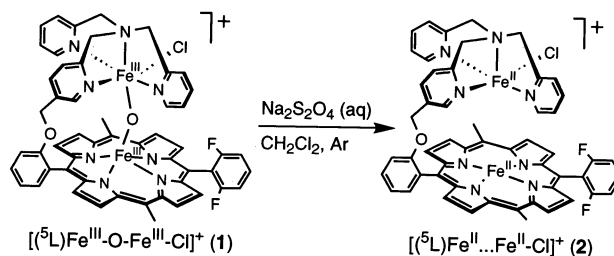
3.1. Syntheses of heme/non-heme diiron(II) complexes

$[(^5\text{L})\text{Fe}^{\text{II}}\cdots\text{Fe}^{\text{II}}\text{-Cl}](\text{ClO}_4)$ (**2a**) and
 $[(^5\text{L})\text{Fe}^{\text{II}}\cdots\text{Fe}^{\text{II}}\text{-Cl}](\text{BAr}^{\text{F}})$ (**2b**)

For modeling the reactivity of the NOR active site with NO or O₂, the synthesis of reduced reactive diiron(II) complexes was needed. Our initial attempts to generate an $[(^5\text{L})\text{Fe}^{\text{II}}\cdots\text{Fe}^{\text{II}}\text{-X}]^+$ species were carried out by adding Fe^{II}Br₂ to the ‘empty tether’ iron(II) complex $[(^5\text{L})\text{Fe}^{\text{II}}]$; this latter species has been previously described [13]. The idea was that Fe^{II}Br₂ can be added directly to this reduced complex to generate the $[(^5\text{L})\text{Fe}^{\text{II}}\cdots\text{Fe}^{\text{II}}\text{-Br}]^+$ species. However, this method did not work well and only impure products (as judged by UV–Vis spectroscopy) could be obtained. The insolubility of Fe^{II}Br₂ probably also contributed to the difficulties encountered.

The second and successful approach was to directly reduce the previously characterized diiron(III) μ -oxo compound $[(^5\text{L})\text{Fe}^{\text{III}}\text{-O-Fe}^{\text{III}}\text{-Cl}]^+$ (**1**) [15]. The counteranion of the parent complex, i.e. $[(^5\text{L})\text{Fe}^{\text{III}}\text{-O-Fe}^{\text{III}}\text{-Cl}](\text{Cl})$ (see Section 2), can be substituted through a simple counterion exchange method, e.g. $[(^5\text{L})\text{Fe}^{\text{III}}\text{-O-Fe}^{\text{III}}\text{-Cl}](\text{Cl})$ is stirred with NaBAr^F to exchange the Cl⁻ counterion for BAr^{F-}. The ¹⁹F NMR spectrum of the resulting $[(^5\text{L})\text{Fe}^{\text{III}}\text{-O-Fe}^{\text{III}}\text{-Cl}](\text{BAr}^{\text{F}})$ (**1b**) complex in CD₂Cl₂ reveals a new peak at –63.4 ppm (s, sh) in addition to the peaks from –106 to –109 ppm. These latter resonances have been

previously assigned as tetraphenylporphyrinate *ortho* and *para* fluorine signals, from examination of spectra of $(^5\text{L})\text{Fe}^{\text{II}}$ ‘empty-tether’ complexes [13]; therefore the new peak was assigned to BAr^{F-}. Subsequent reduction of **1b** is carried out using sodium dithionite in a mixed solvent system, followed by extraction into dichloromethane; precipitation gives the desired product, $[(^5\text{L})\text{Fe}^{\text{II}}\cdots\text{Fe}^{\text{II}}\text{-Cl}](\text{BAr}^{\text{F}})$ (**2b**), in high yield. An analogous procedure was followed in order to generate $[(^5\text{L})\text{Fe}^{\text{II}}\cdots\text{Fe}^{\text{II}}\text{-Cl}](\text{ClO}_4)$ (**2a**). These reduced complexes show characteristic (porphyrinate)Fe^{II} UV–Vis spectra [13], e.g. 424 (Soret) and 544 nm in THF for $[(^5\text{L})\text{Fe}^{\text{II}}\cdots\text{Fe}^{\text{II}}\text{-Cl}](\text{ClO}_4)$ (**2a**).



From ¹H NMR spectroscopy, an iron(II) spin-state solvent dependency is observed for complexes $[(^5\text{L})\text{Fe}^{\text{II}}\cdots\text{Fe}^{\text{II}}\text{-Cl}]^+$ (**2**), Table 1. This is best demonstrated in the behavior of $[(^5\text{L})\text{Fe}^{\text{II}}\cdots\text{Fe}^{\text{II}}\text{-Cl}](\text{BAr}^{\text{F}})$ (**2b**). In non-coordinating solvents (i.e. CD₂Cl₂), the pyrrole resonances are split into four peaks (28–31 ppm) (Fig. 1), typical of a five-coordinate high spin Fe(II) in an unsymmetrical tethered tetraarylporphyrin-

Table 1
Summary of spectroscopic data

	$[(^5\text{L})\text{Fe}^{\text{II}}\cdots\text{Fe}^{\text{II}}\text{-Cl}](\text{ClO}_4)$ (2a)	$[(^5\text{L})\text{Fe}^{\text{II}}\cdots\text{Fe}^{\text{II}}\text{-Cl}](\text{BAr}^{\text{F}})$ (2b)
UV–Vis	424 (Soret), 544 nm ^a 422 (Soret), 532 nm ^b	424 (Soret), 549 nm ^a
¹ H NMR	53–58 (m, pyrrole) ppm ^c	28 (s, pyrrole), 57 (m, pyrrole) ppm ^c 28.7 (s), 28.9 (s), 30.2 (s), 30.6 (s) (all pyrrole), 10.60 (s, py), –10.19 (s, py) ppm ^d
¹⁹ F NMR ^e	–108.11 (br, s), –108.76 (br, s), –112.97 (sh, s), –113.39 (sh, s), –113.80 (sh, s) (all TPP-F) ppm ^f	–63.5 (s, BAr ^{F-}), –104 (br, TPP-F), –105 (br, TPP-F) ppm ^f
MALDI–TOF–MS	$m/z = 1186 (M - \text{ClO}_4)^+$	$m/z = 1186 (M - \text{BAr}^{\text{F}-})^+$
UV–Vis O ₂ intermediate	416 (Soret), 538 nm ^g 420 (Soret), 544 nm ^h	416 (Soret), 538 nm ^g
UV–Vis NO intermediate	414 (Soret), 548 nm ^g	414 (Soret), 546 nm ^g

^a THF.

^b C₂H₅CN.

^c 300 MHz, THF-d₈.

^d 300 MHz, CD₂Cl₂.

^e Referenced to α,α,α -trifluorotoluene.

^f 400 MHz, THF-d₈.

^g THF, –80°C.

^h C₂H₅CN, –80°C.

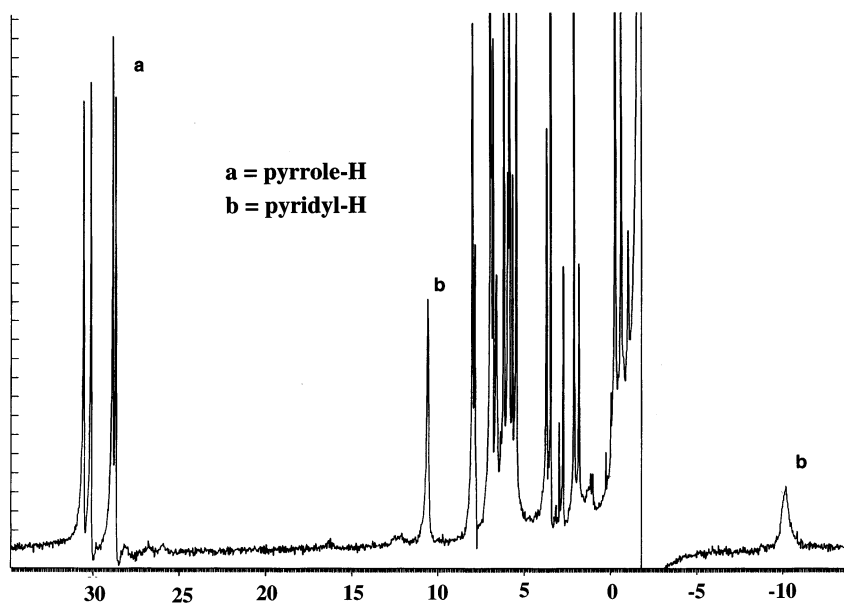


Fig. 1. ^1H NMR spectrum (CD_2Cl_2) of $[(^5\text{L})\text{Fe}^{\text{II}}\cdots\text{Fe}^{\text{II}}\text{-Cl}](\text{BAR}^{\text{F}})$ (**2b**) showing the pyrrole (a) and pyridyl (b) protons.

nate environment [13a]. Additional peaks are observed at 10.6 ppm and upfield at -10.2 ppm. We attribute these latter resonances to protons on one of the pyridyl arms of the tethered TMPA moiety in ^5L , since very similar peaks are observed for $(^6\text{L}/^5\text{L})\text{Fe}(\text{II})$ ‘empty-tether’ complexes [13], where these pyridyl arms are not metal-coordinated and readily available to act as heme axial ligands [13]. Que and co-workers [18] have shown that the pyridyl arms of the $(\text{TMPA})\text{Fe}^{\text{II}}$ moiety undergo facile exchange processes with the solvent in solution. Thus, we suggest that it is possible for a pyridyl arm in $[(^5\text{L})\text{Fe}^{\text{II}}\cdots\text{Fe}^{\text{II}}\text{-Cl}](\text{BAR}^{\text{F}})$ (**2b**) to coordinate to the proximate (heme) $\text{Fe}(\text{II})$.

For $[(^5\text{L})\text{Fe}^{\text{II}}\cdots\text{Fe}^{\text{II}}\text{-Cl}](\text{BAR}^{\text{F}})$ (**2b**) in moderately coordinating solvents such as THF-d_8 , the pyrrole resonances are split into two sets of peaks. One set shifts downfield to 50–60 (m) ppm (similar to $[(^5\text{L})\text{Fe}^{\text{II}}\cdots\text{Cu}^{\text{I}}]^+$ in THF-d_8) [13] and the other set appears at 28.1 as a broad singlet (as for $[(^5\text{L})\text{Fe}^{\text{II}}\cdots\text{Fe}^{\text{II}}\text{-Cl}](\text{BAR}^{\text{F}})$ (**2b**) in CD_2Cl_2 , but without splitting). These downfield pyrrole resonances are consistent with a five-coordinate high spin $\text{Fe}(\text{II})$, but now with the presence of a mixture of species, as there is competition between the pyridyl arm and THF solvent acting as the fifth axial ligand. There is also a weak signal at -9.2 (s) ppm, but the corresponding peak resulting from the coordination of the pyridyl arms to Fe^{II} , at around 11 ppm is absent. For $[(^5\text{L})\text{Fe}^{\text{II}}\cdots\text{Fe}^{\text{II}}\text{-Cl}](\text{ClO}_4)$ (**2a**) in THF-d_8 , it appears that only THF acts as axial ligand, since a high-spin $\text{Fe}(\text{II})$ spectrum is obtained where the pyrrole peaks are split into multiplets at 53–58 ppm. In the strongly coordinating solvent pyridine- d_5 , the pyrrole signals of $[(^5\text{L})\text{Fe}^{\text{II}}\cdots\text{Fe}^{\text{II}}\text{-Cl}](\text{BAR}^{\text{F}})$ (**2b**) shift to the diamagnetic

region, suggesting a hexacoordinate low spin (porphyrinate) $\text{Fe}^{\text{II}}(\text{pyridine})_2$ center is present.

3.2. Reaction of $[(^5\text{L})\text{Fe}^{\text{II}}\cdots\text{Fe}^{\text{II}}\text{-Cl}](\text{ClO}_4)$ (**2a**) and $[(^5\text{L})\text{Fe}^{\text{II}}\cdots\text{Fe}^{\text{II}}\text{-Cl}](\text{BAR}^{\text{F}})$ (**2b**) with dioxygen

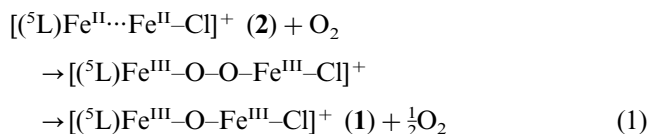
The reactivities of $\text{Fe}(\text{II})$ -containing compounds with dioxygen have been studied extensively [19]. However, previous studies have concentrated on reactions between dioxygen with either exclusively heme or non-heme ferrous compounds only. In addition to nitric oxide chemistry in modeling the active-site reactivity of NOR, reactions of dioxygen with $[(^5\text{L})\text{Fe}^{\text{II}}\cdots\text{Fe}^{\text{II}}\text{-Cl}]^+$ are of interest in understanding the small molecular reactivity of heme/non-heme diiron centers. Also, NOR has been shown to reduce dioxygen [3,9], as mentioned before.

When dioxygen is added directly to $[(^5\text{L})\text{Fe}^{\text{II}}\cdots\text{Fe}^{\text{II}}\text{-Cl}]^+$ at r.t. in THF, the various salt complexes react rapidly and cleanly to form $[(^5\text{L})\text{Fe}^{\text{III}}\text{-O-Fe}^{\text{III}}\text{-Cl}]^+$, as monitored by UV–Vis spectroscopy. No intermediate is observed. However, when $[(^5\text{L})\text{Fe}^{\text{II}}\cdots\text{Fe}^{\text{II}}\text{-Cl}]^+$ reacts with dioxygen in THF or $\text{C}_2\text{H}_5\text{CN}$ at -80°C , a relatively stable ($\sim 2\text{--}3$ h) intermediate can be detected by low-temperature UV–Vis spectroscopy (see Section 2), Fig. 2. This intermediate exhibits a spectrum with a Soret band that is blue-shifted compared to the reduced complex in the same solvent. The characteristics of the O_2 -adducts of diiron(II) complexes under various conditions are: $[(^5\text{L})\text{Fe}^{\text{II}}\cdots\text{Fe}^{\text{II}}\text{-Cl}](\text{ClO}_4)$ (**2a**) in THF, 416 (Soret) and 538 nm; $\text{C}_2\text{H}_5\text{CN}$, 420 (Soret) and 544 nm; $[(^5\text{L})\text{Fe}^{\text{II}}\cdots\text{Fe}^{\text{II}}\text{-Cl}](\text{BAR}^{\text{F}})$ (**2b**) in THF, 416 (Soret) and 538 nm, Fig. 2. The shifts are consistent with previous

observations in the literature [19e] for metallo-porphyrin complexes reacting with O₂ and converting them from Fe(II) to Fe(III). The product formed from either decomposition over time at –80°C, or by warming the solution to r.t., is identified as [(⁵L)Fe^{III}–O–Fe^{III}–Cl]⁺, by UV–Vis spectroscopy (Fig. 2). ¹H NMR spectroscopic comparisons of the product isolated by oxygenation of **2** also proves that the product formed from exposing [(⁵L)Fe^{II}…Fe^{II}–Cl]⁺ (**2**) to dioxygen is indeed [(⁵L)Fe^{III}–O–Fe^{III}–Cl]⁺ (**1**). While no direct evidence is available at this time, we suggest that the intermediate in this reaction could be an intra-molecularly formed μ-1,2-peroxo diiron(III) complex, [(⁵L)Fe^{III}–O–O–Fe^{III}–Cl]⁺, similar to Fe–O–O–Cu species proposed to form in heme-Cu cytochrome *c* oxidase models [21].

There is a possibility that the observed O₂-adduct may just be a simple porphyrin Fe–O₂ complex which can be stable at low temperature [20]. Further studies (e.g. by ¹H NMR spectroscopy) are needed. And, there are other plausible types of peroxo bound intermediates that may represent the λ_{max} ~ 416 nm intermediate (Fig. 2) observed in the O₂ reaction with [(⁵L)Fe^{II}…Fe^{II}–Cl]⁺ (**2**). Namely, these are an inter-molecular (non-heme Fe–O–O–Fe non-heme) species [19a,22], an inter-molecular (heme Fe–O–O–Fe heme) complex [19b,23], a mononuclear ferric porphyrin peroxo [24] species, or a complex with an inter-molecular (heme Fe–O–O–Fe non-heme) interaction. However, a closer look suggests that the first three possibilities may be ruled out simply on the basis of their respective reported UV–Vis spectra. Dimeric non-heme Fe(III) peroxo, dimeric heme Fe(III) peroxo, and monomeric ferric peroxo complexes generally exhibit very different UV–Vis spectra than the intermediate detected in this work [22–24]. Also,

previous work has shown that ((TMPA)Fe–O–O–Fe(TMPA)) was not detected even at –80°C [18]. Furthermore, if a dimeric heme–heme Fe(III)₂ peroxo complex is the intermediate, the autoxidation [23a] of this complex would instead probably lead to the bis-porphyrinate μ-oxo tetranuclear species [Cl–Fe…(⁵L)Fe^{III}–O–Fe^{III}(⁵L)…Fe–Cl]ⁿ⁺ as the final product; this should exhibit bands at around 399 (Soret) and 560 nm in its UV–Vis spectroscopy [25,26]. Lastly, this intermediate lacks the stability that is observed in monomeric ferric peroxo complexes [24]. Inter-molecular (heme Fe–O–O–Fe non-heme) binding cannot be ruled out, but seems unlikely as both steric considerations and low complex concentration used would make an intra-molecular interaction more favorable. Thus, we suggest that the reaction which occurs here is:



Mechanisms by which μ-peroxo diiron(III) complexes can thermally decompose to μ-oxo diiron(III) compounds have been described for heme complexes [27], and more recently for non-heme diiron species [19a,22c,28]. A number of mechanisms are observed or postulated.

3.3. Reactions of [(⁵L)Fe^{II}…Fe^{II}–Cl](ClO₄) (**2a**) and [(⁵L)Fe^{II}…Fe^{II}–Cl](BAR^F) (**2b**) with nitric oxide at low and high complex concentrations

There is considerable literature on the binding of nitric oxide to (heme)Fe(II)/(III) complexes, synthesized through various routes [29–32], and an NO bound non-heme Fe(II) complex has also been isolated and characterized [33]. However, there still lacks an accurate structural and functional model for NOR. Recently, a triiron(II) complex that contains both heme and non-heme metal centers [34] has been synthesized, but [(⁵L)Fe^{II}…Fe^{II}–Cl]⁺ (**2**) probably depicts a more precise active site model for the reduced NOR active site.

UV–Vis spectroscopic monitoring of the reaction of [(⁵L)Fe^{II}…Fe^{II}–Cl]⁺ (**2**) at low complex concentration (i.e. < 10 μM) with NO at –80°C in THF shows that there is the formation of an intermediate (see Table 1 and Fig. 3) which is stable at low temperature. Interestingly, the λ_{max} of the band observed complies more closely with a [(heme)Fe^{II}–(NO)₂] and other hexa-coordinated (heme)Fe(II) complex than a penta-coordinated (heme)Fe(II) complexes [30,31]. UV–Vis spectral properties of the non-heme iron center within the observed species cannot be ascertained, as extinction coefficient due to this chromophore would be much lower than the

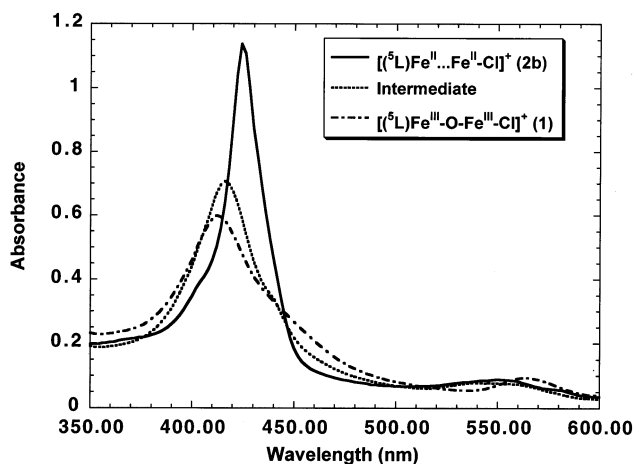


Fig. 2. Low temperature UV–Vis spectra (–80°C, THF) following the reactions of [(⁵L)Fe^{II}…Fe^{II}–Cl](BAR^F) (**2b**) (λ_{max} = 424, 549 nm) with O₂ to form an intermediate (λ_{max} = 416, 538 nm), and final μ-oxo product [(⁵L)Fe^{III}–O–Fe^{III}–Cl](BAR^F) (**1b**) (λ_{max} = 412, 567 nm). See text for further details.

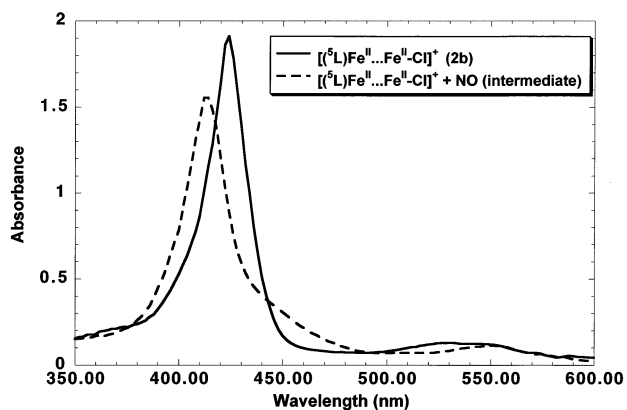
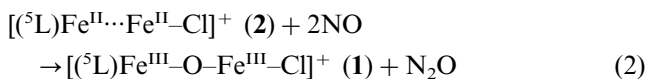


Fig. 3. Low temperature UV-Vis spectra (-80°C , THF) following the reactions of $[(^5\text{L})\text{Fe}^{\text{II}}\cdots\text{Fe}^{\text{II}}\text{-Cl}]^+(\mathbf{2b})$ ($\lambda_{\text{max}} = 424, 549 \text{ nm}$) with NO to form an intermediate ($\lambda_{\text{max}} = 414, 546 \text{ nm}$). See text for further details.

heme iron center [33]. Upon warming the solution of **2** which has been exposed to NO to r.t., the observed intermediate converts to the μ -oxo complex $[(^5\text{L})\text{Fe}^{\text{III}}\text{-O-Fe}^{\text{III}}\text{-Cl}]^+(\mathbf{1})$, as judged by the UV-Vis changes.

Reactions of this type have been observed in Cu(I) compounds [35], in which oxo-bridged dicopper(II) complexes have formed from Cu(I) compounds reacting with NO. The concomitant generation of nitrous oxide, N_2O , was observed. In the case of reaction of $[(^5\text{L})\text{Fe}^{\text{II}}\cdots\text{Fe}^{\text{II}}\text{-Cl}]^+$ with NO, it is possible that the reaction may proceed in a similar fashion:



However, at the concentrations used for these spectroscopic observations, we found it too difficult to utilize gas chromatography (GC) to analyze to see if any gaseous products (i.e. N_2O) are formed.

At higher complex concentrations (i.e. $\geq 0.1 \text{ mM}$), where the concentration of any gaseous product is enough to be readily detected by GC analysis, reaction of $[(^5\text{L})\text{Fe}^{\text{II}}\cdots\text{Fe}^{\text{II}}\text{-Cl}]^+(\mathbf{2})$ with NO produced both N_2O and NO_2 , as detected by GC analysis of the head-space gases produced. The major metal complex product is a red solid, which shows a UV-Vis spectrum (when redissolved in THF) which is identical to that observed in the warmed reaction solution, showing bands at 412 (Soret) and 545 nm. The ^1H NMR spectrum (300 MHz, THF- d_8) of this product has pyrrole peaks (64.6 (s, br), 58.5 (s, br), 53.6 (s) and 50.7 (s) ppm) which are indicative of a high spin (heme)Fe(II) species [13]. The peaks from the non-heme protons ((300 MHz, THF- d_8): 145.3 (s), 64.7 (s), 46.6 (s), 45.5 (s), and 22.5 (s)) suggest that the non-heme Fe(II) is also high spin [18]. Solution FT-IR (Fig. 4) spectroscopy provides support

for the presence of a penta-coordinated [(heme)-Fe^{II}-NO] structure. In THF, the FT-IR spectrum exhibits a peak at 1660 cm^{-1} , which conforms to observations for other (porphyrinate)Fe(II) compounds containing a bent, terminal NO moiety [29,32b,36]. Resonance Raman spectroscopy data obtained on the final product (from reaction of NO with $[(^5\text{L})\text{Fe}^{\text{II}}\cdots\text{Fe}^{\text{II}}\text{-Cl}](\text{BAr}^{\text{F}})$ (**2b**)) are also consistent with a pentacoordinated ferrous-NO complex. The Fe-N and N-O stretches observed at $521 (\Delta(^{15}\text{N}^{18}\text{O}) = -11 \text{ cm}^{-1})$ and 1657 cm^{-1} , respectively, are very similar to other five-coordinate low-spin ferrous heme nitrosyl complexes such as (tetraphenylporphyrinate)iron(II)-NO in THF [37].

One final observation about the red product of NO reaction with $[(^5\text{L})\text{Fe}^{\text{II}}\cdots\text{Fe}^{\text{II}}\text{-Cl}]^+(\mathbf{2})$ is that this compound is air-sensitive. In THF solvent, exposure to O_2 readily converts it to $[(^5\text{L})\text{Fe}^{\text{III}}\text{-O-Fe}^{\text{III}}\text{-Cl}]^+(\mathbf{1})$, as monitored by UV-Vis spectroscopy. Mechanistic studies have not been carried out, but this reaction may proceed by dioxygen displacement of bound NO, followed by oxidation of the iron centers to the highly stable μ -oxo product **1**. Another possibility is that O_2 oxidation of the heme-NO produces nitrite or nitrate, which is followed by oxygen transfer [38].

3.4. Possible mechanism of observed reactions

Future studies will be required to probe the reaction between $[(^5\text{L})\text{Fe}^{\text{II}}\cdots\text{Fe}^{\text{II}}\text{-Cl}]^+(\mathbf{2})$ and nitric oxide in order to understand the mechanism for the production of N_2O and NO_2 , seemingly a disproportionation of NO. Such metal complex mediated disproportionation reactions are known, although they usually result in the trapping of the NO_2 fragment in a metal-coordinated nitrite (NO_2^-) complex [39]. Nitrous oxide production from reaction of iron compounds with NO is not uncommon; reduced myoglobin [40] and the non-heme ribonucleotide reductase [41] proteins have both been

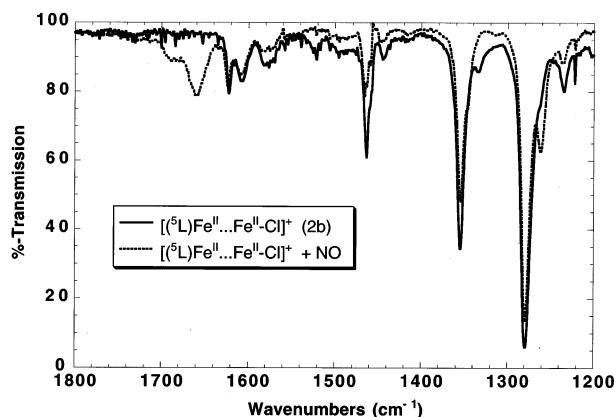
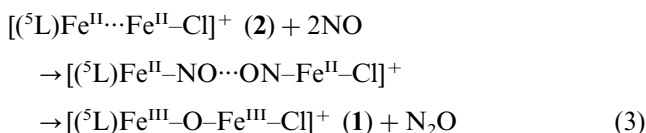


Fig. 4. FT-IR spectra of $[(^5\text{L})\text{Fe}^{\text{II}}\cdots\text{Fe}^{\text{II}}\text{-Cl}](\text{BAr}^{\text{F}})$ (**2b**) and the reaction product with NO, suggesting the formation of a (heme)ferrous-NO complex ($\nu_{\text{N-O}} 1660 \text{ cm}^{-1}$).

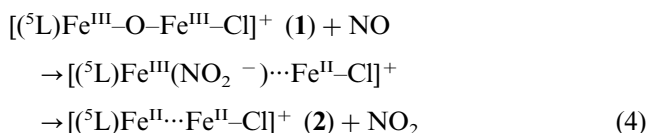
demonstrated to react with NO to form N₂O. The evolutionary related enzyme CcO has also been shown to reduce NO to N₂O [10]. Different mechanisms have been proposed for the formation of N₂O by NOR in bacterial denitrification [1,2,6]. We suggest that the mechanism for the reduction of NO to N₂O in the present chemical system involves the reaction of NO with the two coordinatively unsaturated iron(II) centers in **2**, followed by coupling of two metal bound nitrosyls, thus allowing for N–N bond formation. The reaction is postulated to follow a 2-electron reduction reaction, with a driving force for reaction provided by μ -oxo formation in **1**:



However, N₂O could not be observed as the reaction product, because of the low concentrations used to observe the stoichiometric reaction; further studies are required.

As mentioned, the generation of NO₂ from reaction with nitric oxide has not been as common as N₂O in biological and model systems. A literature example is the reaction of oxidized CcO (under aerobic conditions) with NO [10]. There are, however, many Fe–heme systems [30,32] that undergo oxidative reactions of NO to give NO₂⁻. In the present system, NO may react with the μ -oxo complex [({}^5L)Fe^{III}-O-Fe^{III}-Cl]⁺ (**1**) (formed via Eq. (3)), giving a heme iron(III)–nitrite

species, which then releases NO₂(g), thereby reforming **2**:



The product reduced complex [({}^5L)Fe^{II}⋯Fe^{II}-Cl]⁺ (**2**) can then react with any NO that is present and the reaction cycle can continue, Fig. 5.

We note that a [(heme)Fe(III)]₂O complex is known to react with NO to form [(heme)Fe^{III}(NO₂)(NO)] [32]. We also have separately determined that tetrakis(2,6-difluorophenyl)-porphyrinate-iron(II) [42] is able to disproportionate NO; GC analysis of reaction of with NO (under conditions of concentration identical to those carried out for **2**) shows that both N₂O and NO₂ are produced. This observation thus makes it less clear as to what role is played by the non-heme iron center in **1** and **2**, for these NO_x reactions. Also, the reaction scheme given in Fig. 5 implies that a catalytic cycle exists. Further experiments are needed to quantitate the relative and total amount of N₂O and NO₂ that are produced in the reaction of **2** with NO, but the observations discussed make it clear that the cycle (and catalysis) may not occur at low concentrations (where only the μ -oxo complex [({}^5L)Fe^{III}-O-Fe^{III}-Cl]⁺ (**1**) is formed, *vide supra*), and/or breaking of the cycle occurs as the red solid (i.e. iron nitrosyl complex) is produced. We note that relative NO concentrations are known to affect the reactivity of NOR and CcO

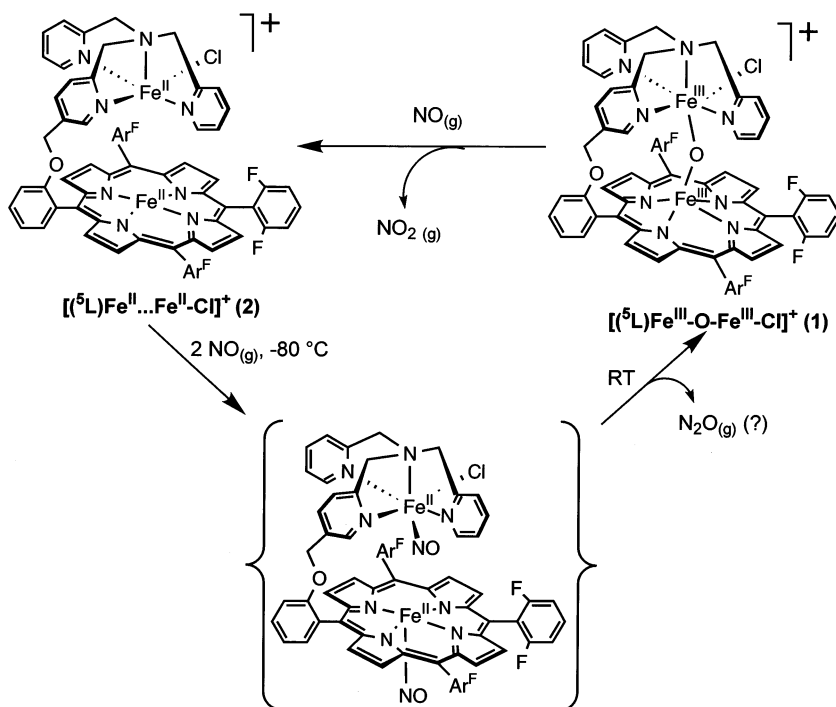


Fig. 5. Scheme involving NO reactions of [({}^5L)Fe^{II}-O-Fe^{II}-Cl]⁺ (**1**) and [({}^5L)Fe^{II}⋯Fe^{II}-Cl]⁺ (**2**). See text for further details.

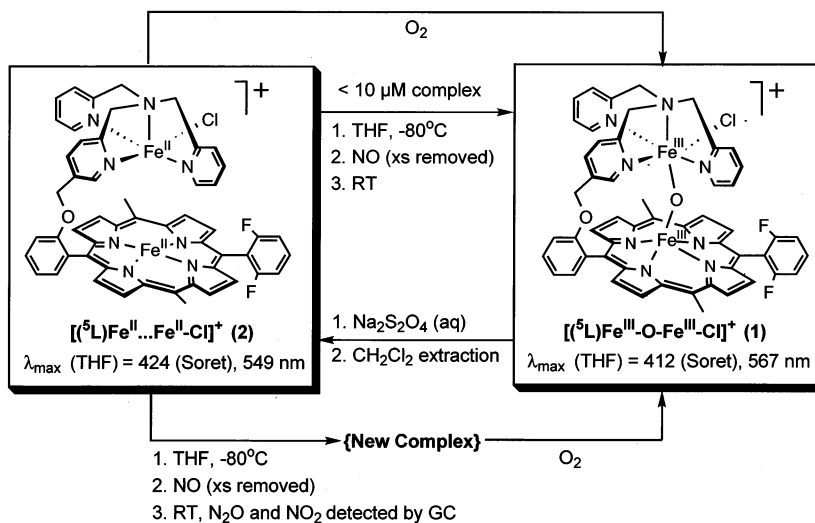


Fig. 6. Summary of the chemical interconversions of $[(^5L)Fe^{II}\cdots Fe^{II}-Cl]^+$ (**1**) and $[(^5L)Fe^{III}-O-Fe^{III}-Cl]^+$ (**2**), including reactions with O_2 and NO.

[2,10b,36b], and there are many situations [43] where relative reagent concentrations strongly influence the mechanism or course of reaction.

4. Conclusions and summary

Novel, highly reactive heme/non-heme diiron(II) compounds, $[(^5L)Fe^{II}\cdots Fe^{II}-Cl]^+$ (**2**), have been synthesized by reduction of the previously characterized μ -oxo complex $[(^5L)Fe^{III}-O-Fe^{III}-Cl]^+$ (**1**) and characterized as either a perchlorate (**2a**) or tetraarylborate (BAR^{F} ; **2b**) anion complexes. These species may prove to be useful in the functional modeling of NOR with its heme/non-heme diiron active site center. Complex **2** exhibits interesting properties, in which the spin state of the heme-Fe(II) can change according to solvent. In a non-coordinating solvent, a pyridyl arm from the tether (bound to the non-heme iron) can coordinate to the heme center. This is not observed in the Fe/Cu analog system [13a].

The interconversion chemistry of **1** and **2**, involving reactions of **2** with dioxygen or nitric oxide, is summarized in Fig. 6. $[(^5L)Fe^{II}\cdots Fe^{II}-Cl]^+$ (**2**) readily reacts with dioxygen, and an intermediate that is postulated to be a peroxo-diiron(III) complex, can be observed at -80°C . Upon warming, the intermediate proceeds to form the μ -oxo complex $[(^5L)Fe^{III}-O-Fe^{III}-Cl]^+$ (**1**). The reduced complex also reacts at low concentration with NO to form $[(^5L)Fe^{III}-O-Fe^{III}-Cl]^+$ (**1**), presumably giving off N_2O . Further studies are required. However, when the NO and complex reagent concentrations are increased, a reaction proceeds which generates both N_2O and NO_2 . The metal complex product isolated exhibits properties of a penta-coordinated NO bound heme-Fe(II) complex, based on data collected

from UV-Vis, ^1H NMR, IR, and resonance Raman spectroscopies.

Thus, $[(^5L)Fe^{II}\cdots Fe^{II}-Cl]^+$ (**2**) serves as a first generation model for the reduced heme/non-heme diiron(II) NOR active site, with its demonstrated interesting reactivities with O_2 and NO. To better understand the intricacies of the chemistry involved, the mechanism of both NO and O_2 reactions, the nature of the intermediates, the effects of concentration of the reactants and the identity of the isolated complex are under further investigation. Future studies will also involve generation and study of analogs or derivatives of **1** and **2**.

Acknowledgements

We appreciate the financial support from the National Institutes of Health (K.D.K., GM28962; R.J.C., GM54882; P.M.-L., GM34468 to Professor Thomas M. Loehr, Oregon Graduate Institute).

References

- [1] W.G. Zumft, *Microbiol. Mol. Biol. Rev.* 61 (1997) 533 and Refs. therein.
- [2] B.A. Averill, *Chem. Rev.* 96 (1996) 2951.
- [3] N. Sakurai, T. Sakurai, *Biochemistry* 36 (1997) 13 809.
- [4] J. Hendriks, A. Warne, U. Gohlke, T. Haltia, C. Ludovici, M. Lübben, M. Saraste, *Biochemistry* 37 (1998) 13 102.
- [5] P. Girsch, S. de Vries, *Biochim. Biophys. Acta* 1318 (1997) 202.
- [6] P. Moënne-Loccoz, S. de Vries, *J. Am. Chem. Soc.* 120 (1998) 5147.
- [7] T. Sakurai, N. Sakurai, H. Matsumoto, S. Hirota, O. Yamauchi, *Biochem. Biophys. Res. Commun.* 251 (1998) 248.
- [8] M.R. Cheesman, W.G. Zumft, A.J. Thomson, *Biochemistry* 37 (1998) 3994.
- [9] G. Stubauer, A. Giuffrè, M. Brunori, P. Sarti, *Biochem. Biophys. Res. Commun.* 245 (1998) 459.

- [10] (a) G.H. Brudvig, T.H. Stevens, S.I. Chan, *Biochemistry* 19 (1980) 5275. (b) X.-J. Zhao, V. Sampath, W.S. Caughey, *Biochem. Biophys. Res. Commun.* 212 (1995) 1054.
- [11] (a) T. Fujiwara, Y. Fukumori, *J. Bacteriol.* 178 (1996) 1866. (b) G. Stubauer, A. Giuffè, M. Brunori, P. Sarti, *Biochem. Biophys. Res. Commun.* 245 (1998) 459.
- [12] M.-A. Kopf, K.D. Karlin, in: B. Meunier (Ed.), *Biomimetic Oxidations*, Imperial College Press, London, 2000 (Ch. 7), 309–362.
- [13] (a) T.D. Ju, R.A. Ghiladi, D.-H. Lee, G.P.F. van Strijdonck, A.S. Woods, R.J. Cotter, V.G. Young Jr., K.D. Karlin, *Inorg. Chem.*, 38 (1999) 2244. (b) R.A. Ghiladi, T.D. Ju, D.-H. Lee, P. Moënné-Loccoz, S. Kaderli, Y.-M. Neuhold, A.D. Zuberbühler, A.S. Woods, R.J. Cotter, K.D. Karlin, *J. Am. Chem. Soc.* 121 (1999) 9885.
- [14] H.V. Obias, G.P.F. van Strijdonck, M. Ralle, N.J. Blackburn, K.D. Karlin, *J. Am. Chem. Soc.* 120 (1998) 9696.
- [15] C.F. Martens, N.N. Murthy, H.V. Obias, K.D. Karlin, *J. Chem. Soc., Chem. Commun.* (1996) 629.
- [16] (a) Z. Tyeklár, R.R. Jacobson, N. Wei, N.N. Murthy, J. Zubieta, K.D. Karlin, *J. Am. Chem. Soc.* 115 (1993) 2677. (b) K.D. Karlin, M.S. Haka, R.W. Cruse, G.J. Meyer, A. Farooq, Y. Gultneh, J.C. Hayes, J. Zubieta, *J. Am. Chem. Soc.* 110 (1988) 1196.
- [17] M. Brookhart, B. Grant, A.F. Volpe Jr., *Organometallics* 11 (1992) 3920.
- [18] S. Ménage, Y. Zang, M.P. Hendrich, L. Que Jr., *J. Am. Chem. Soc.* 114 (1992) 7786.
- [19] For a few examples, including Refs. cited therein, see the following: (a) A.L. Feig, S.J. Lippard, *Chem. Rev.* 94 (1994) 759. (b) L. Que, Jr., R.Y.N. Ho, *Chem. Rev.* 96 (1996) 2607. (c) A.L. Balch, *Inorg. Chim. Acta* 198 (1992) 297. (d) M. Sono, M.P. Roach, E.D. Coulter, J.H. Dawson, *Chem. Rev.* 96 (1996) 2841. (e) G.B. Jameson, J.B. Ibers, in: I. Bertini, H.B. Gray, S.J. Lippard, J.S. Valentine (Eds.), *Bioinorganic Chemistry*, University Science, Mill Valley, CA, 1994 (Chapter 4), pp. 167–252.
- [20] L. Latos-Grazynski, R.-J. Cheng, G.N. La Mar, A.L. Balch, *J. Am. Chem. Soc.* 104 (1982) 5992.
- [21] (a) T. Sasaki, N. Nakamura, Y. Naruta, *Chem. Lett.* (1998) 351. (b) J.P. Collman, P.C. Herrmann, B. Boitrel, X. Zhang, T.A. Eberspacher, L. Fu, J. Wang, D.L. Rousseau, E.R. Williams, *J. Am. Chem. Soc.* 116 (1994) 9783. (c) J.P. Collman, L. Fu, P.C. Herrmann, X. Zhang, *Science* 275 (1997) 949. (d) J.P. Collman, R. Schwenninger, M. Rapta, M. Bröring, L. Fu, *Chem. Commun.* (1999) 137. (e) J.P. Collman, M. Rapta, M. Bröring, L. Raptova, R. Schwenninger, B. Boitrel, L. Fu, M. L'Her, *J. Am. Chem. Soc.* 121 (1999) 1387.
- [22] (a) E. Kimura, M. Kodama, R. Machida, K. Ishizu, *Inorg. Chem.* 21 (1982) 595. (b) Y. Dong, S. Ménage, B.A. Brennan, T.E. Elgren, H.G. Jang, L.L. Pearce, L. Que, Jr., *J. Am. Chem. Soc.* 115 (1993) 1851. (c) A.L. Feig, M. Becker, S. Schindler, R. van Eldik, S.J. Lippard, *Inorg. Chem.* 35 (1996) 2590. (d) N. Kitajima, N. Tamura, H. Amagai, H. Fukui, Y. Mora-oka, Y. Mizutani, T. Kitagawa, R. Mathur, K. Heerwegh, C.A. Reed, C.R. Randall, L. Que, Jr., K. Tatsumi, *J. Am. Chem. Soc.* 116 (1994) 9071.
- [23] (a) D.-H. Chin, G.N. La Mar, A.L. Balch, *J. Am. Chem. Soc.* 102 (1980) 4344. (b) A.L. Balch, Y.-W. Chan, R.-J. Cheng, G.N. La Mar, L. Latos-Grazynski, M.W. Renner, *J. Am. Chem. Soc.* 106 (1984) 7779.
- [24] M. Selke, M.F. Sisemore, R.Y.N. Ho, D.L. Wertz, J.S. Valentine, *J. Mol. Catal.* 117 (1997) 71.
- [25] H.V. Obias, Ph.D. Dissertation, Johns Hopkins University, 1998.
- [26] K.D. Karlin, A. Nanthakumar, S. Fox, N.N. Murthy, N. Ravi, B.H. Huynh, R.D. Orosz, E.P. Day, *J. Am. Chem. Soc.* 116 (1994) 4753.
- [27] A.L. Balch, *Inorg. Chim. Acta* 198–200 (1992) 297.
- [28] A.L. Feig, A. Masschelein, A. Bakac, S.J. Lippard, *J. Am. Chem. Soc.* 119 (1997) 334.
- [29] W.R. Scheidt, M.K. Ellison, *Acc. Chem. Res.* 32 (1999) 350.
- [30] (a) B.B. Wayland, L.W. Olsen, *J. Am. Chem. Soc.* 96 (1974) 6037. (b) W.R. Scheidt, M.E. Frisse, *J. Am. Chem. Soc.* 97 (1975) 17. (c) D.S. Bohle, P. Debrunner, J.P. Fitzgerald, B. Hansert, C.-H. Hung, A.J. Thomson, *J. Chem. Soc., Chem. Commun.* (1997) 91.
- [31] H. Nasri, M.K. Ellison, S. Chen, B.H. Huynh, W.R. Scheidt, *J. Am. Chem. Soc.* 119 (1997) 6274.
- [32] (a) M.F. Settin, J.C. Fanning, *Inorg. Chem.* 27 (1988) 1431. (b) M.K. Ellison, C.E. Schulz, W.R. Scheidt, *Inorg. Chem.* 38 (1999) 100.
- [33] Y.-M. Chiou, L. Que Jr., *Inorg. Chem.* 34 (1995) 3270.
- [34] X.-X. Zhang, P. Fuhrmann, S.J. Lippard, *J. Am. Chem. Soc.* 120 (1998) 10260.
- [35] P.P. Paul, K.D. Karlin, *J. Am. Chem. Soc.* 113 (1991) 6331.
- [36] X.D. Ding, A. Weichsel, J.F. Anderson, T.K. Shokhireva, C. Belfour, A.J. Pierik, B.A. Averill, W.r. Montfort, F.A. Walker, *J. Am. Chem. Soc.* 121 (1999) 128.
- [37] (a) I.-K. Choi, Y. Liu, D.W. Feng, K.-J. Paeng, M.D. Ryan, *Inorg. Chem.* 30 (1991) 1832. (b) L.A. Lipscomb, B.-S. Lee, N.-T. Yu, *Inorg. Chem.* 32 (1993) 281.
- [38] P. Guillaume, H.L.K. Wah, M. Postel, *Inorg. Chem.* 30 (1991) 1828.
- [39] (a) J.L. Schneider, S.M. Carrier, C.E. Ruggiero, V.G. Young, Jr., W.B. Tolman, *J. Am. Chem. Soc.* 120 (1998) 11408. (b) K.J. Franz, S.J. Lippard, *J. Am. Chem. Soc.* 120 (1998) 9034.
- [40] M. Bayachou, R. Lin, W. Cho, P.J. Farmer, *J. Am. Chem. Soc.* 120 (1998) 9888.
- [41] C.J. Haskin, N. Ravi, J.B. Lynch, E. Münck, L. Que Jr., *Biochemistry* 34 (1995) 11090.
- [42] (a) A. Nanthakumar, S. Fox, K.D. Karlin, *J. Chem. Soc., Chem. Commun.* (1995) 499. (b) M.-A. Kopf, Y.-M. Neuhold, A.D. Zuberbühler, K.D. Karlin, *Inorg. Chem.* 38 (1999) 3043.
- [43] See, for example: (a) S. Mahapatra, S. Kaderli, A. Llobet, Y.-M. Neuhold, T. Palanché, J.A. Halfen, V.G. Young, Jr., T.A. Kaden, L. Que, Jr., A.D. Zuberbühler, W.B. Tolman, *Inorg. Chem.* 36, (1997) 6343. (b) T.D. Ju, K.B. Capps, G.C. Roper, R.F. Lang, C.D. Hoff, *Inorg. Chim. Acta* 270 (1998) 488.